

Cite this: DOI: 10.1039/xxxxxxxxxx

The rotational spectrum of ^{15}ND . Isotopic-independent Dunham-type analysis of the imidogen radical[†]

Mattia Melosso^a, Luca Bizzocchi^{b,*}, Filippo Tamassia^c, Claudio Degli Esposti^a, Elisabetta Canè^c, and Luca Dore^{a,*}

Received Date

Accepted Date

DOI: 10.1039/xxxxxxxxxx

www.rsc.org/journalname

The rotational spectrum of ^{15}ND in its ground electronic $X^3\Sigma^-$ state has been observed for the first time. Forty-three hyperfine-structure components belonging to the ground and $v = 1$ vibrational states have been recorded with a frequency-modulation millimeter-/submillimeter-wave spectrometer. These new measurements, together with the ones available for the other isotopologues NH, ND, and ^{15}NH , have been simultaneously analysed using the Dunham model to represent the ro-vibrational, fine, and hyperfine energy contributions. The least-squares fit of more than 1500 transitions yielded an extensive set of isotopically independent U_{lm} parameters plus 13 Born–Oppenheimer Breakdown coefficients Δ_{lm} . As an alternative approach, we performed a Dunham analysis in terms of the most abundant isotopologue coefficients Y_{lm} and some isotopically dependent Born–Oppenheimer Breakdown constants δ_{lm} [R. J. Le Roy, *J. Mol. Spectrosc.* **194**, 189 (1999)]. The two fits provide results of equivalent quality. The Born–Oppenheimer equilibrium bond distance for the imidogen radical has been calculated [$r_e^{\text{BO}} = 103.606721(13)$ pm] and zero point energies have been derived for all the isotopologues.

1 Introduction

The imidogen radical has been the subject of many spectroscopic, computational and astrophysical studies. This diatomic radical belongs to the first-row hydrides, is commonly observed in the combustion products of nitrogen-bearing compounds^{1,2}, and is also an intermediate in the formation process of ammonia in the interstellar medium (ISM)³. The main isotopologue of imidogen, NH, has been detected in a wide-variety of environments, from the Earths' atmosphere to astronomical objects, such as comets⁴, many types of stars^{5,6} including the Sun^{7,8}, diffuse clouds⁹, massive star-forming (SF) regions¹⁰ and, very recently, in prestellar cores¹¹. Also its deuterated counterpart ND has been identified

in the ISM, towards the young solar-mass protostar IRAS16293¹² and in the prestellar core 16293E¹¹.

A lot of studies have been devoted to the origin of interstellar imidogen and different formation models have been proposed to explain its observed abundance in various sources. Two main formation routes have been devised for the NH radical: from the electronic recombination of NH^+ and NH_2^+ , intermediates in the synthesis of interstellar ammonia^{13,14} starting with N^+ or, alternatively, via dissociative recombination of N_2H^+ ¹⁵. However, the mechanism of NH production in the ISM is still debated¹⁰, and grain-surface processes might also play a significant role¹⁶. Imidogen, together with other light hydrides, often appears in the first steps of chemical networks leading to more complex N-bearing molecules. Its observation thus provides crucial constraints for the chemical modeling of astrophysical sources¹⁷. Also the rare isotopologues of this radical yield important astrochemical insights. Being proxies for N and D isotopic fractionation processes, they may help to trace the evolution of gas and dust during the star formation, thus shedding light on the link between Solar System materials and the parent ISM¹⁸. This is particularly relevant for nitrogen, whose molecular isotopic compositions exhibits large and still unexplained variations^{19,20}. Measuring the isotopic ratios in imidogen provides useful complementary information on the already measured H/D, $^{14}\text{N}/^{15}\text{N}$ in ammonia (including the $^{15}\text{NH}_2\text{D}$ species²¹).

As far as the laboratory work is concerned, there is a substan-

* Corresponding author.

^a Dipartimento di Chimica “Giacomo Ciamician”, Università di Bologna, Via F. Selmi 2, 40126 Bologna (Italy). E-mail: mattia.melosso2@unibo.it, claudio.degliesti@unibo.it luca.dore@unibo.it

^b Center for Astrochemical Studies, Max-Planck-Institut für extraterrestrische Physik, Gießenbachstr. 1, 85748 Garching bei München (Germany) E-mail: bizzocchi@mpe.mpg.de

^c Dipartimento di Chimica Industriale “Toso Montanari”, Università di Bologna, Viale del Risorgimento 4, 40136 Bologna (Italy). E-mail: filippo.tamassia@unibo.it, elisabetta.cane@unibo.it

[†] Electronic Supplementary Information (ESI) available: The .LIN and .PAR files for the SPFIT program are provided for both the single-species and multi-isotopologues fits. A reformatted list of all the transitions used in the Dunham-type analysis, together with their residuals from the final fit, is also included as ESI. See DOI: 10.1039/c8cp04498h

tial amount of spectroscopic data for the most abundant species and less extensive measurements for ^{15}NH and ND . A detailed description of the spectroscopic studies of imidogen can be found in the latest experimental works on NH^{22} , $^{15}\text{NH}^{23}$, and ND^{24} . It has to be noticed that no experimental data or theoretical computations were available in literature for the doubly substituted species ^{15}ND up to date. In this work, we report the first observation of its pure rotational spectrum in the ground electronic state $X^3\Sigma^-$ recorded up to 1.068 THz. A limited number of new transition frequencies for the isotopologues NH and ND in the $\nu = 1$ excited state have also been measured in the course of the present investigation. This new set of data, together with the literature data for NH , ^{15}NH and ND , have been analysed in a global multi-isotopologue fit to give a comprehensive set of isotopically independent spectroscopic parameters. Thanks to the high precision of the measurements, several Born–Oppenheimer Breakdown (BOB) constants (Δ_{lm}) could be determined from a Dunham-type analysis. The alternative Dunham approach proposed by Le Roy²⁵ has been also employed. In this case, the results are expressed in terms of the parent species coefficients Y_{lm} plus some isotopically dependent BOB constants (δ_{lm}).

Finally, very accurate equilibrium bond distances r_e (including the Born–Oppenheimer bond distance r_e^{BO}) and Zero-Point Energies (ZPE) for each isotopologue have been computed from the determined spectroscopic constants.

2 Experiments

The rotational spectrum of ^{15}ND radical in its ground vibronic state $X^3\Sigma^-$ has been recorded with a frequency-modulation millimeter-/submillimeter-wave spectrometer. The primary source of radiation was constituted by a series of Gunn diodes (Radiometer Physics GmbH, J. E. Carlstrom Co.) emitting in the range 80–134 GHz, whose frequency is stabilized by a Phase-Lock-Loop (PLL) system. The PLL allowed the stabilization of the Gunn oscillator with respect to a frequency synthesizer (Schomandl ND 1000), which was driven by a 5 MHz rubidium frequency standard. Higher frequencies were obtained by using passive multipliers (RPG, $\times 6$ and $\times 9$). The frequency modulation of the output radiation was realized by sine-wave modulating at 6 kHz the reference signal of the wide-band Gunn synchronizer. The signal was detected by a liquid-helium-cooled InSb hot electron bolometer (QMC Instr. Ltd. type QFI/2) and then demodulated at $2f$ by a lock-in amplifier. The experimental uncertainties of present measurements are between 40 and 80 kHz in most cases, up to 500 kHz for a few disturbed lines.

The ^{15}ND radical was formed in a glow-discharge plasma with the same apparatus employed to produce other unstable and rare species (e.g., ND_2 ²⁶ and $^{15}\text{N}_2\text{H}^+$ ²⁷). The optimum production was attained in a DC discharge of a mixture of $^{15}\text{N}_2$ (5–7 mTorr) and D_2 (1–2 mTorr) in Ar as buffer gas (15 mTorr). Typically, a voltage of 1 kV and a current of 60 mA were employed. The absorption cell was cooled down at ca. -190°C by liquid-nitrogen circulation.

Table 1 Spectroscopic constants determined for ^{15}ND in the ground and $\nu = 1$ vibrational states.

Constant	Unit	$\nu = 0$	$\nu = 1$
B_ν	/ MHz	261083.4809(96)	253597.797(24)
D_ν	/ MHz	14.3906(13)	14.3906 ^a
λ_ν	/ MHz	27544.852(22)	27544.852 ^a
γ_ν	/ MHz	-876.139(15)	-841.674(46)
$\gamma_{N\nu}$	/ MHz	0.1241(20)	0.1241 ^a
$b_{F,\nu}(^{15}\text{N})$	/ MHz	-26.519(20)	-25.944(41)
$c_\nu(^{15}\text{N})$	/ MHz	95.154(56)	94.48(30)
$C_{l,\nu}(^{15}\text{N})$	/ MHz	-0.124(14)	-0.124 ^a
$b_{F,\nu}(\text{D})$	/ MHz	-10.062(21)	-10.524(42)
$c_\nu(\text{D})$	/ MHz	14.236(78)	13.18(22)
$eQq_\nu(\text{D})$	/ MHz	0.271(93)	0.271 ^a
σ_w^b			0.84
rms	/ MHz		0.080
no. of lines		34	9

Notes.

Number in parentheses are the 1σ statistical errors in unit of the last quoted digit. ^(a) Parameter held fixed in the fit. ^(b) Fit standard deviation.

3 Analysis

3.1 Effective Hamiltonian

From a spectroscopic point of view, imidogen is a free radical with a $X^3\Sigma^-$ ground electronic state and exhibits a fine structure due to the dipole-dipole interaction of the two unpaired electron spins and to the magnetic coupling of the molecular rotation with the total electron spin. The couplings of the various angular momenta in NH are described more appropriately by Hund’s case (*b*) scheme

$$\mathbf{J} = \mathbf{N} + \mathbf{S}, \quad (1)$$

where \mathbf{N} represents the pure rotational angular momentum. Each fine-structure level is thus labeled by J, N quantum numbers, where $J = N + 1, N, N - 1$. For $N = 0$, only one component ($J = 1$) exists. Inclusion of the nitrogen and hydrogen hyperfine interactions leads to the couplings

$$\mathbf{F}_1 = \mathbf{J} + \mathbf{I}_N, \quad \mathbf{F} = \mathbf{F}_1 + \mathbf{I}_H. \quad (2)$$

For each isotopologue in a given ro-vibronic state, the effective Hamiltonian can be written as

$$\mathbf{H} = \mathbf{H}_{rv} + \mathbf{H}_{fs} + \mathbf{H}_{hfs} \quad (3)$$

where \mathbf{H}_{rv} , \mathbf{H}_{fs} and \mathbf{H}_{hfs} are the ro-vibrational, fine- and hyperfine-structure Hamiltonians, respectively:

$$\mathbf{H}_{rv} = G_\nu + B_\nu \mathbf{N}^2 - D_\nu \mathbf{N}^4 + H_\nu \mathbf{N}^6 + L_\nu \mathbf{N}^8 + M_\nu \mathbf{N}^{10} \quad (4)$$

$$\mathbf{H}_{fs} = \frac{2}{3} (\lambda_\nu + \lambda_{N\nu} \mathbf{N}^2) (3S_z^2 - \mathbf{S}^2) + (\gamma_\nu + \gamma_{N\nu} \mathbf{N}^2) \mathbf{N} \cdot \mathbf{S} \quad (5)$$

$$\begin{aligned} \mathbf{H}_{\text{hfs}} = & \sum_i b_{F,v}(i) \mathbf{I}_i \cdot \mathbf{S} + \sum_i c_v(i) \left(I_{iz} S_z - \frac{1}{3} \mathbf{I}_i \cdot \mathbf{S} \right) \\ & + \sum_i eQq_v(i) \frac{(3I_{iz}^2 - \mathbf{I}_i^2)}{4I_i(2I_i - 1)} + \sum_i C_{I,v}(i) \mathbf{I}_i \cdot \mathbf{N} \end{aligned} \quad (6)$$

Here, G_v is the pure vibrational energy, B_v the rotational constant, D_v , H_v , L_v , and M_v the centrifugal distortion parameters up to the fifth power in the $\hat{\mathbf{N}}^2$ expansion, λ_v and λ_{Nv} are the electron spin–spin interaction parameter and its centrifugal distortion coefficient; γ_v and γ_{Nv} are the electron spin–rotation constant and its centrifugal distortion coefficient, respectively. The constants $b_{F,v}$ and c_v are the isotropic (Fermi contact interaction) and anisotropic parts of the electron spin–nuclear spin coupling, eQq_v represents the electric quadrupole interaction and $C_{I,v}$ is the nuclear spin–rotation parameter. In Eq. (6) the index i runs over the different nuclei present in a given isotopologue. The four nuclear spins are: $I = 1/2$ for H and ^{15}N and $I = 1$ for D and ^{14}N .

3.2 Multi-isotopologue Dunham models

In order to treat the data of all the available isotopologues in a global analysis, it is convenient to adopt a Dunham-type expansion³⁵. The ro-vibrational energy levels are given by the equation:

$$E_{\text{rv}}(v, N) = \sum_{l,m} Y_{lm} \left(v + \frac{1}{2} \right)^l [N(N+1)]^m. \quad (7)$$

The fine- and hyperfine-structure parameters [i.e., λ_v , λ_{Nv} , γ_v , γ_{Nv} , $b_{F,v}$, c_v , eQq_v , and $C_{I,v}$ in Eqs. (5)–(6)], are given by analogous expansions:

$$y(v, N) = \sum_{l,m} \mathcal{Y}_{lm} \left(v + \frac{1}{2} \right)^l [N(N+1)]^m, \quad (8)$$

where $y(v, N)$ represents the effective value of the parameter y in the ro-vibrational level labeled by (v, N) , and \mathcal{Y}_{lm} are the coefficients of its Dunham-type expansion*.

The spectroscopic constants of Eqs. (4)–(6) can be expressed in terms of the Dunham coefficients Y_{lm} and \mathcal{Y}_{lm} . For example, the constants G_v , B_v , and D_v , of the ro-vibrational Hamiltonian are given by the following expansions:

$$G_v = \sum_{l=0} Y_{l0} \left(v + \frac{1}{2} \right)^l, \quad (9a)$$

$$B_v = \sum_{l=0} Y_{l1} \left(v + \frac{1}{2} \right)^l, \quad (9b)$$

$$D_v = \sum_{l=0} Y_{l2} \left(v + \frac{1}{2} \right)^l. \quad (9c)$$

Each fine- and hyperfine-structure constant is also expressed by suitable expansions. For example, the electron spin-rotation constant and its centrifugal dependence in a given vibrational state v

can be expressed as:

$$\gamma_v = \sum_{l=0} \gamma_{l0} \left(v + \frac{1}{2} \right)^l, \quad (10a)$$

$$\gamma_{Nv} = \sum_{l=0} \gamma_{l1} \left(v + \frac{1}{2} \right)^l, \quad (10b)$$

where γ_{l0} and γ_{l1} are the \mathcal{Y}_{lm} constants of Eq. 8 relative to the spin-rotation interaction. For a given isotopologue α , a specific set of Dunham constants $Y_{lm}^{(\alpha)}$ and $\mathcal{Y}_{lm}^{(\alpha)}$ is defined. Such constants can be described in terms of isotopically invariant parameters using the known reduced mass dependences given by^{36,37}

$$Y_{lm}^{(\alpha)} = U_{lm} \mu_\alpha^{-(l/2+m)} \left[1 + m_e \left(\frac{\Delta_{lm}^{\text{N}}}{M_{\text{N}}^{(\alpha)}} + \frac{\Delta_{lm}^{\text{H}}}{M_{\text{H}}^{(\alpha)}} \right) \right], \quad (11a)$$

$$\mathcal{Y}_{lm}^{(\alpha)} = U_{lm}^y \mu_\alpha^{-(l/2+m+p)} \left[1 + m_e \left(\frac{\Delta_{lm}^{y,\text{N}}}{M_{\text{N}}^{(\alpha)}} + \frac{\Delta_{lm}^{y,\text{H}}}{M_{\text{H}}^{(\alpha)}} \right) \right], \quad (11b)$$

where $M_X^{(\alpha)}$ (with $X = \text{N, H}$) are the atomic masses, μ_α is the reduced mass of the α isotopologue, and m_e is the electron mass. U_{lm} and U_{lm}^y are isotopically invariant Dunham constants, whereas Δ_{lm}^{X} and $\Delta_{lm}^{y,\text{X}}$ are unitless coefficients which account for the Born–Oppenheimer Breakdown^{37,38}. In Eq. (11b), $p = 0$ for $y = \lambda, b_F, c, eQq$, while $p = 1$ for $y = \gamma, C_I$. This extra μ^{-1} factor in the mass scaling is needed to account for the intrinsic N^2 dependence of the spin–rotation constants³⁹. Here, the unknowns are the U_{lm} , U_{lm}^y coefficients and the corresponding Δ_{lm}^{X} and $\Delta_{lm}^{y,\text{X}}$ BOB corrections.

An alternative approach has been proposed by LeRoy²⁵, where one isotopologue (usually the most abundant one) is chosen as reference species ($\alpha = 1$), and the Dunham parameters $Y_{lm}^{(\alpha)}$ and $\mathcal{Y}_{lm}^{(\alpha)}$ of any other species are obtained by the following mass scaling

$$Y_{lm}^{(\alpha)} = \left[Y_{lm}^{(1)} + \frac{\Delta M_{\text{N}}}{M_{\text{N}}^{(\alpha)}} \delta_{lm}^{\text{N}} + \frac{\Delta M_{\text{H}}}{M_{\text{H}}^{(\alpha)}} \delta_{lm}^{\text{H}} \right] \left(\frac{\mu_1}{\mu_\alpha} \right)^{(l/2+m)}, \quad (12a)$$

$$\mathcal{Y}_{lm}^{(\alpha)} = \left[\mathcal{Y}_{lm}^{(1)} + \frac{\Delta M_{\text{N}}}{M_{\text{N}}^{(\alpha)}} \delta_{lm}^{y,\text{N}} + \frac{\Delta M_{\text{H}}}{M_{\text{H}}^{(\alpha)}} \delta_{lm}^{y,\text{H}} \right] \left(\frac{\mu_1}{\mu_\alpha} \right)^{(l/2+m+p)}. \quad (12b)$$

Here, $\Delta M_X = M_X^{(\alpha)} - M_X^{(1)}$ (with $X = \text{N, H}$) are the mass differences produced by the isotopic substitution, with respect to the reference species, and the BOB corrections are described by the new δ_{lm}^{X} and $\delta_{lm}^{y,\text{X}}$ coefficients. These are related to the dimensionless Δ_{lm}^{X} of Eqs. 11 through the simple relation

$$\Delta_{lm}^{\text{X}} = \delta_{lm}^{\text{X}} \frac{M_X^{(1)}}{m_e} \left(Y_{lm}^{(1)} + \delta_{lm}^{\text{N}} + \delta_{lm}^{\text{H}} \right)^{-1}. \quad (13)$$

Albeit formally equivalent, this latter parametrisation was introduced to overcome a number of deficiencies of the traditional treatment which were pointed out by Watson³⁷ and Tiemann⁴⁰, and its features are discussed in great detail in the original paper²⁵. An obvious advantage of the alternative mass scaling of Eqs. (12) is that the fitted coefficients are all expressed in

* This (v, N) -factorisation is possible because all the angular momentum operators multiplying the coefficients of Eqs. (5) and (6) commute with purely vibrational operators and with N^2 .

frequency units and are directly linked to the familiar spectroscopic parameters of the reference isotopologue (e.g., $Y_{10}^{(1)} \approx \omega_e$, $Y_{20}^{(1)} \approx -\omega_e x_e$, $Y_{01}^{(1)} \approx B_e$, $Y_{11}^{(1)} \approx -\alpha_e$, etc.). Furthermore, the BOB contributions are accounted for using purely additive terms thus reducing the correlations among the parameters.

4 Results

4.1 ^{15}ND spectrum

For the previously unobserved ^{15}ND species, we have recorded 34 lines for the ground vibrational state and 9 lines for the $\nu = 1$ state. They include the complete fine-structure of the $N = 1 \leftarrow 0$ transition and the strongest fine-components of the $N = 2 \leftarrow 1$ transition for the ground state (see Figure 1), and the $\Delta J = 0, +1$ components of the $N = 1 \leftarrow 0$ transition for the $\nu = 1$ state. The corresponding transition frequencies were fitted to the Hamiltonian of Eqs. (4)–(6) using the SPFIT analysis program⁴¹. Because of the small number of transitions detected for the $\nu = 1$ state, some of the spectroscopic parameters for this state could not be directly determined in the least-squares fit and were constrained to the corresponding ground state values. The two sets of constants for $\nu = 0$ and $\nu = 1$ states are reported in Table 1. The list of observed frequencies, along with the residuals from the single-species fit, is given in Table 2. In addition, the .LIN and .PAR input files for the SPFIT program are included in the supplementary material †.

4.2 Multi-isotopologue Dunham fit

In this work, we carried out a multi-isotopologue Dunham fit of the imidogen radical in its $X^3\Sigma^-$ ground electronic state using our newly measured transition frequencies for the doubly substituted ^{15}ND variant plus all the available rotational and ro-vibrational data for the NH, ^{15}NH and ND species. To take into account the different experimental precision, each datum was given a weight inversely proportional to the square of its estimated measurement error, $w = 1/\sigma^2$. The σ values adopted for the present measurements have been discussed in § 2, while for literature data, we retained the values provided in each original work.

The content of the data set and the relevant bibliographic references are summarised in Table 3. In total, the data set contains 1563 ro-vibrational transitions which correspond to 1201 distinct frequencies. These data were fitted to the multi-isotopologue model described in §§ 3.1–3.2, using both traditional [Eqs. (11)] and LeRoy [Eqs. (12)] mass scaling schemes to describe the Dunham-type parameters (Y_{lm} and γ_{lm}) of each isotopic species.

The analysis was performed using a custom PYTHON code which uses the SPFIT program⁴¹ as computational core. Briefly, the scripting routine reads the atomic masses, the spin multiplicities, and the Y_{lm} constants for the reference species. Then, the SPFIT parameter file (.PAR) is set up by defining several sets of spectroscopic constants (one for each isotopologue/vibrational state), taking into account the mass scaling factors. The SPFIT lines file (.LIN) is created by collecting the experimental data. In this process, half integer quantum numbers are rounded up and a "quantum number state" is assigned to each isotopologue in a given vibrational state, in conformity with the SPFIT format. At

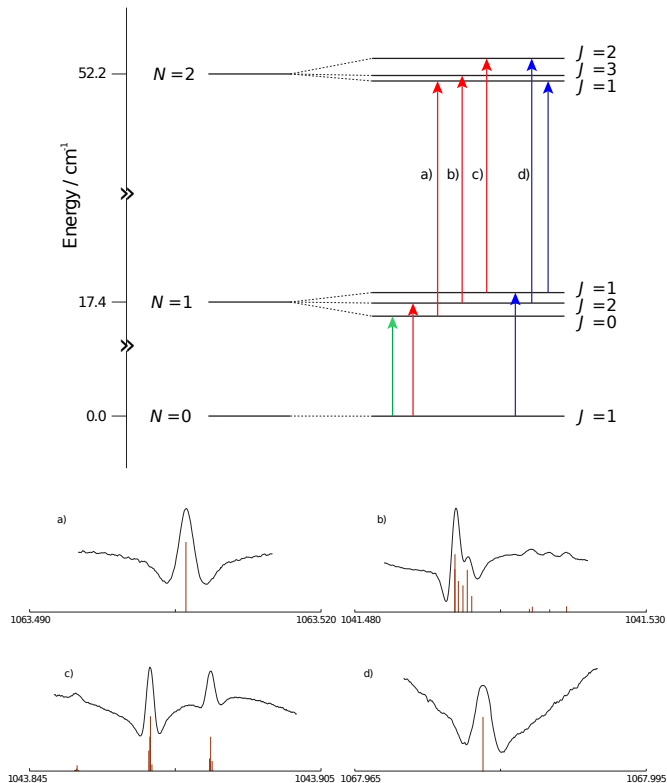


Fig. 1 Upper panel: energy levels scheme of ^{15}ND in the ground vibrational state. The hyperfine-structure is not shown. The arrows mark the transitions observed in this study: $\Delta J = +1$ (red), $\Delta J = 0$ (blue), and $\Delta J = -1$ (green). Lower panel: spectral recordings for the transitions marked with the labels a, b, c and d showing the corresponding hyperfine structure. The brown sticks represent the positions and the intensities of the hyperfine components computed from the spectroscopic parameters of Table 1.

the end of the least-squares optimisation, the SPFIT output is post-processed, and the final parameters list is reformatted in the same fashion of the initial input data set. The atomic masses used were taken from the Wang *et al.*⁴² compilation. The optimised parameters are reported in Tables 4 and 5, while the complete list of all the fitted data, together with the residuals from the multi-isotopologue analysis, is provided as supplementary material (the .LIN and .PAR files are also provided) †.

5 Discussion

5.1 Spectroscopic parameters

From the multi-isotopologue analysis we obtained a highly satisfactory fit. Its quality can be evaluated in several ways. First of all, we were able to reproduce the input data within their estimated uncertainties: the overall standard deviation of the weighted fit is $\sigma = 0.89$, and the root-mean-square deviations of the residuals computed separately for the rotational and ro-vibrational data are of the same order of magnitude of the corresponding measurements error, $\text{RMS}_{\text{ROT}} = 0.107 \text{ MHz}$ and $\text{RMS}_{\text{VIBROT}} = 3.4 \times 10^{-3} \text{ cm}^{-1}$, respectively. Then, the various sets of Y_{lm} for a given m constitute a series whose coefficients decrease in magnitude for increasing values of the index l , as expected for a rapidly converging Dunham-type expansion. In

general, most of the determined coefficients have a relative error lower than 5%. Higher errors are observed only for those constants with high l -index and this is due to the smaller number of transitions available for highly vibrationally excited states. Finally, the Kratzer⁴³ and Pekeris⁴⁴ relation can also be used as a yardstick to assess the correct treatment of the Born–Oppenheimer Breakdown effects. Using the formula⁴⁵

$$Y_{02} \simeq \frac{4Y_{01}^3}{Y_{10}^2}, \quad (14)$$

we obtained for Y_{02} a value of 51.54051 MHz which compares well with the fitted one of 51.44722(91) MHz.

5.2 Equilibrium bond distance

The precision yielded by the high-resolution spectroscopic technique led to a very accurate determination of the equilibrium bond length r_e for the imidogen radical. The rotational measurements of a diatomic molecule in its ground vibrational state ($v = 0$) allow the determination of precise value of r_0 , which includes the zero point vibrational contributions and differs from r_e . This latter is determinable from the rotational spectrum in at least one vibrationally excited state. In the present analysis, data of four isotopic species in several vibrational excited states have been combined, allowing for a very precise determination of r_e for each isotopologue α . The equilibrium bond distance is given by:

$$r_e^{(\alpha)} = \sqrt{\frac{N_a h}{8\pi^2} \frac{1}{B_e^{(\alpha)} \mu_a}}. \quad (15)$$

where $N_a h$ is the molar Planck constant. Actually, the values of $B_e^{(\alpha)}$ differ from those of $Y_{01}^{(\alpha)}$ obtained from the Dunham-type analysis. This discrepancy should be ascribed to a small contribution, expressed by⁴⁵:

$$Y_{01} = B_e + \Delta Y_{01}^{(\text{Dunh})} = B_e + \beta_{01} \left(\frac{B_e^3}{\omega_e^2} \right), \quad (16)$$

with

$$\beta_{01} = Y_{10}^2 \left(\frac{Y_{21}}{4Y_{01}^3} \right) + 16a_1 \left(\frac{Y_{20}}{3Y_{01}} \right) - 8a_1 - 6a_1^2 + 4a_1^3, \quad (17)$$

and

$$a_1 = \frac{Y_{11}}{3\sqrt{-Y_{02}Y_{01}}} - 1. \quad (18)$$

From Eq. (15), it is evident that the bond length r_e assumes different values for each isotopologue. On the contrary, by substituting the product $B_e^{(\alpha)} \mu_a$ with U_{01} , one obtains an isotopically independent equilibrium bond length r_e^{BO} . In the present case, r_e^{BO} takes the value of 103.606721(13) pm. In Table 6, this result is compared with the equilibrium bond distances calculated from the B_e of each isotopologue NH, ¹⁵NH, ND, and ¹⁵ND. In this case, B_e was obtained by correcting the corresponding Y_{01} constant according to Eqs. (16)–(18). It should be noticed that the values differ at sub-picometre level but these differences, even if small, are detectable thanks to the high-precision of rotational measurements.

The experimental value derived for r_e^{BO} has been compared with a theoretically best estimate obtained following the prescriptions of Refs. 46,47. A composite calculation have been carried out considering basis-set extrapolation, core-correlation effects, and inclusion of higher-order corrections due to the use of the full coupled-cluster singles and doubles, augmented by a perturbative treatment of triple excitation [CCSD(T)] model

$$\text{fc-CCSD(T)/cc-pV}\infty\text{Z} + \Delta\text{core/cc-pCV5Z} + \Delta\text{T/cc-pVTZ}.$$

The computation have been performed using CFOUR⁴⁸. From this theoretical procedure we obtained $r_e^{\text{theor}} = 103.5915$ pm (see also Table 6), which is in very good agreement with the experimentally derived value, the discrepancy being 15 fm.

5.3 Born–Oppenheimer Breakdown

The BOB coefficients Δ_{lm}^X determined in the present analysis account for the small inaccuracies of the Born–Oppenheimer approximation in describing the ro-vibrational energies of the imidogen radical. For the rotational constant ($\approx Y_{01}$), it is possible to identify three different contributions to the corresponding BOB parameter⁴⁹

$$\begin{aligned} \Delta_{01}^X &= \left(\Delta_{01}^X \right)^{\text{ad}} + \left(\Delta_{01}^X \right)^{\text{nad}} + \left(\Delta_{01}^X \right)^{\text{Dunh}} \\ &= \left(\Delta_{01}^X \right)^{\text{ad}} + \frac{(\mu g_J)_{X'}}{m_p} + \frac{\Delta Y_{01}^{(\text{Dunh})} \mu}{m_e B_e}, \end{aligned} \quad (19)$$

namely an adiabatic contribution, a non-adiabatic term, and a Dunham correction, respectively. The last two terms on the right side of Eq. (19) can be computed from purely experimental quantities: $\left(\Delta_{01}^X \right)^{\text{Dunh}}$ arises from the use of a Dunham expansion and contains the term $\Delta Y_{01}^{(\text{Dunh})}$ of Eq. (16), whereas $\left(\Delta_{01}^X \right)^{\text{nad}}$ depends on the mixing of the electronic ground state with nearby electronic excited states, and can be estimated from the molecular electric dipole moment μ and the rotational g_J factors³⁸. The adiabatic term can be simply computed as the difference between the experimental Δ_{01}^X and the terms $\left(\Delta_{01}^X \right)^{\text{Dunh}}$ and $\left(\Delta_{01}^X \right)^{\text{nad}}$.

Tiemann *et al.*⁴⁰ found that the adiabatic term $\left(\Delta_{01}^X \right)^{\text{ad}}$ basically depends on the corresponding X atom rather than on the particular molecular species. Hence, it is interesting to derive this contribution in order to compare the results obtained for different molecules and to verify the reliability of the empirical fitting procedure.

All the contributions of Eq. (19) are collected in Table 7. The non-adiabatic contribution has been computed using the literature value of the dipole moment⁵⁰ $\mu = 1.389$ D and the ground state g_J value estimated from a laser magnetic resonance study⁵¹, $g_J = 0.001524$.

From the adiabatic contribution to the Born–Oppenheimer Breakdown coefficients for the rotational constants, $\left(\Delta_{01}^X \right)^{\text{ad}}$, one may derive the corresponding correction to the equilibrium bond distance, a quantity which can also be accessed by *ab initio* computations. From our Eq. (11a) and Eq. (6) of Ref. 52, the follow-

ing equality is obtained

$$\Delta R_{\text{ad}} = -\frac{r_e}{2} \left[\frac{m_e}{M_{\text{N}}} \left(\Delta_{01}^{\text{N}} \right)^{\text{ad}} + \frac{m_e}{M_{\text{H}}} \left(\Delta_{01}^{\text{H}} \right)^{\text{ad}} \right]. \quad (20)$$

The adiabatic correction to the equilibrium bond distance, ΔR_{ad} , can be theoretically estimated through the computation of the adiabatic bond distance, i.e., the minimum of the potential given by the sum of the Born–Oppenheimer potential augmented by the diagonal Born–Oppenheimer corrections (DBOC)⁵². The difference between the equilibrium bond distances calculated with and without DBOC, with tight convergence limits, performed at the CCSD/cc-pCVnZ level ($n = 3, 4, 5$), yielded $\Delta R_{\text{ad}} = 0.026$ pm. This value is in very good agreement with the purely experimental one obtained by Eq. (20) which results 0.020 pm, thus providing a confirmation for the validity of our data treatment.

5.4 Zero-point Energy

The results of our analysis make possible to estimate the zero-point energy (ZPE) for each isotopologue from the Dunham’s constants Y_{lm} with $m = 0$, namely:

$$G(0) = \sum_{l=0} Y_{l0} \left(\frac{1}{2} \right)^l. \quad (21)$$

As we determined anharmonicity constants up to the sixth order, the ZPE is derived with a negligible truncation bias⁵³ from the expression:

$$G(0) = Y_{00} + \frac{Y_{10}}{2} - \frac{Y_{20}}{4} + \frac{Y_{30}}{8} + \frac{Y_{40}}{16} + \frac{Y_{50}}{32} + \frac{Y_{60}}{64}. \quad (22)$$

The Y_{00} constant present in the Dunham-type expansions is not experimentally accessible. Its value can be estimated, to a good approximation, through⁵³

$$Y_{00} \simeq \frac{B_e}{4} + \frac{\alpha_e \omega_e}{12B_e} + \frac{\alpha_e^2 \omega_e^2}{12^2 B_e^3} - \frac{\omega_e x_e}{4}. \quad (23)$$

The value for the main isotopologue NH is $1.9987(12) \text{ cm}^{-1}$. The values obtained for the ZPE of the four isotopologues are collected in Table 8. For comparison, the values of literature are also reported. Our results agree well with those reported in the literature⁵³, but our precision is more than one order of magnitude higher. The errors on our ZPE values are *ca.* $1 \times 10^{-3} \text{ cm}^{-1}$ and were calculated taking into account the error propagation

$$\sigma_f^2 = g^T V g \quad (24)$$

where σ_f^2 is the variance in the function f (i.e., Eq. (22) in the present case) of the set of parameters Y_{l0} , whose variance-covariance matrix is V , with the i^{th} element in the vector g being $\frac{\partial f}{\partial Y_i}$.

Discrepancies of $\sim 2 \text{ cm}^{-1}$ are observed by comparing our data with those reported in Ref. 54 because their definition of the ZPE does not include the term Y_{00} , which is non-negligible for light molecules⁵³. These newly determined values should be used in the calculation of the exoergicity values ΔE of chemical reactions relevant in fractionation processes.

6 Conclusions

In this work the pure rotational spectrum of ^{15}ND in its ground electronic $X^3\Sigma^-$ state has been recorded for the first time using a frequency-modulation submillimeter-wave spectrometer. A global fit, including all previously reported rotational and ro-vibrational data for the other isotopologues of the imidogen radical, has been performed and yielded a comprehensive set of Dunham coefficients. Moreover, the Born–Oppenheimer Breakdown constants have been determined for 13 parameters and also the adiabatic contribution of the terms Δ_{01}^{N} and Δ_{01}^{H} were evaluated and compared to theoretical estimates. The present analysis enables to predict rotational and ro-vibrational spectra of any isotopic variant of NH at a high level of accuracy and to assist further astronomical searches of imidogen. From our results, very accurate values of the equilibrium bond distances r_e and the vibrational Zero-Point Energies for the different isotopologues have been derived.

Acknowledgements

This work was supported by Italian MIUR (PRIN 2015 "STARS in the CAOS") and by the University of Bologna (RFO funds).

References

- 1 M. Alexander, P. Dagdigan, M. E. Jacox, C. Kolb, C. Melius, H. Rabitz, M. Smooke and W. Tsang, *Prog. Energy Combust. Sci.*, 1991, **17**, 263–296.
- 2 J. A. Miller and C. T. Bowman, *Prog. Energy Combust. Sci.*, 1989, **15**, 287–338.
- 3 R. Wagenblast, D. A. Williams, T. J. Millar and L. A. M. Nejad, *Mon. Not. R. Astron. Soc.*, 1993, **260**, 420.
- 4 P. Feldman, K. Fournier, V. Grinin and A. Zvereva, *Astrophys. J.*, 1993, **404**, 348–355.
- 5 J. L. Schmitt, *Publ. Astron. Soc. Pac.*, 1969, **81**, 657.
- 6 S. Ridgway, D. Carbon, D. Hall and J. Jewell, *Astrophys. J. Supp.*, 1984, **54**, 177–209.
- 7 N. Grevesse, D. Lambert, A. Sauval, E. Van Dishoeck, C. Farmer and R. Norton, *Astron. Astrophys.*, 1990, **232**, 225–230.
- 8 M. Geller, C. Farmer, R. Norton, A. Sauval and N. Grevesse, *Astron. Astrophys.*, 1991, **249**, 550–552.
- 9 K. Meyer, DM & Roth, *Astrophys. J.*, 1991, **376**, L49–L52.
- 10 C. M. Persson, J. H. Black, J. Cernicharo, J. Goicoechea, G. Hassel, E. Herbst, M. Gerin, M. De Luca, T. Bell, A. Coutens *et al.*, *Astron. Astrophys.*, 2010, **521**, L45.
- 11 Bacmann, A., Daniel, F., Caselli, P., Ceccarelli, C., Lis, D., Vastel, C., Dumouchel, F., Lique, F. and Caux, E., *Astron. Astrophys.*, 2016, **587**, A26.
- 12 A. Bacmann, E. Caux, P. Hily-Blant, B. Parise, L. Pagani, S. Bottinelli, S. Maret, C. Vastel, C. Ceccarelli, J. Cernicharo *et al.*, *Astron. Astrophys.*, 2010, **521**, L42.
- 13 E. Herbst, D. DeFrees and A. McLean, *Astrophys. J.*, 1987, **321**, 898–906.
- 14 E. Galloway, ET & Herbst, *Astron. Astrophys.*, 1989, **211**, 413–418.

- 15 W. D. Geppert, R. Thomas, J. Semaniak, A. Ehlerding, T. J. Millar, F. Österdahl, M. af Ugglas, N. Djurić, A. Paál and M. Larsson, *Astrophys. J.*, 2004, **609**, 459.
- 16 P. T. O'Neill, S. Viti and D. A. Williams, *Astron. Astrophys.*, 2002, **388**, 346–354.
- 17 R. Le Gal, P. Hily-Blant, A. Faure, G. Pineau des Forêts, C. Rist and S. Maret, *Astron. Astrophys.*, 2014, **562**, A83.
- 18 J. Aléon, *Astrophys. J.*, 2010, **722**, 1342–1351.
- 19 B. Marty, M. Chaussidon, R. C. Wiens, A. J. G. Jurewicz and D. S. Burnett, *Science*, 2011, **332**, 1533.
- 20 E. Füri and B. Marty, *Nature Geoscience*, 2015, **8**, 515–522.
- 21 M. Gerin, N. Marcelino, N. Biver, E. Roueff, L. H. Coudert, M. Elkeurti, D. C. Lis and D. Bockelée-Morvan, *Astron. Astrophys.*, 2009, **498**, L9–L12.
- 22 R. Ram and P. Bernath, *J. Mol. Spectrosc.*, 2010, **260**, 115–119.
- 23 L. Bizzocchi, M. Melosso, L. Dore, C. Degli Esposti, F. Tamassia, D. Prudenzeno, V. Lattanzi, J. Laas, S. Spezzano, B. Giuliano, C. Endres and P. Caselli, *Astrophys. J.*, 2018, **863**, 3.
- 24 L. Dore, L. Bizzocchi, C. Degli Esposti and F. Tamassia, *Mol. Phys.*, 2011, **109**, 2191–2198.
- 25 R. J. Le Roy, *J. Mol. Spectrosc.*, 1999, **194**, 189–196.
- 26 M. Melosso, C. Degli Esposti and L. Dore, *Astrophys. J. Supp.*, 2017, **233**, 15.
- 27 L. Dore, L. Bizzocchi, E. S. Wirström, C. Degli Esposti, F. Tamassia and S. B. Charnley, *Astron. Astrophys.*, 2017, **604**, A26.
- 28 J. Flores-Mijangos, J. M. Brown, F. Matsushima, H. Odashima, K. Takagi, L. R. Zink and K. M. Evenson, *J. Mol. Spectrosc.*, 2004, **225**, 189–195.
- 29 F. Lewen, S. Brünken, G. Winnewisser, M. Šimečková and Š. Urban, *J. Mol. Spectrosc.*, 2004, **226**, 113–122.
- 30 T. Bernath, Peter F & Amano, *J. Mol. Spectrosc.*, 1982, **95**, 359–364.
- 31 S. Saito and M. Goto, *Astrophys. J.*, 1993, **410**, L53–L55.
- 32 S. Takano, T. Klaus and G. Winnewisser, *J. Mol. Spectrosc.*, 1998, **192**, 309–319.
- 33 P. Ram, RS & Bernath, *J. Mol. Spectrosc.*, 1996, **176**, 329–336.
- 34 S. Bailleux, M. Martin-Drumel, L. Margulès, O. Pirali, G. Włodarczyk, P. Roy, E. Roueff, M. Gerin, A. Faure and P. Hily-Blant, *Astron. Astrophys.*, 2012, **538**, A135.
- 35 J. L. Dunham, *Phys. Rev.*, 1932, **41**, 721–731.
- 36 A. H. M. Ross, R. S. Eng and H. Kildal, *Opt. Comm.*, 1974, **12**, 433–438.
- 37 J. K. G. Watson, *J. Mol. Spectrosc.*, 1980, **80**, 411–421.
- 38 J. K. G. Watson, *J. Mol. Spectrosc.*, 1973, **45**, 99–113.
- 39 J. M. Brown and J. K. G. Watson, *J. Mol. Spectrosc.*, 1977, **65**, 65–74.
- 40 E. Tiemann, H. Arnst, W. Stieda, T. Törring and J. Hoefl, *Chem. Phys.*, 1982, **67**, 133–138.
- 41 H. M. Pickett, *J. Mol. Spectrosc.*, 1991, **148**, 371–377.
- 42 M. Wang, G. Audi, F. G. Kondev, W. J. Huang, S. Naimi and X. Xu, *Chinese Physics C*, 2017, **41**, 030003.
- 43 A. Kratzer, *Z. Physics*, 1920, **3**, 289.
- 44 C. L. Pekeris, *Phys. Rev.*, 1934, **45**, 98.
- 45 W. Gordy and R. L. Cook, *Microwave molecular spectra*, Wiley, 1984.
- 46 M. Heckert, M. Kállay, D. P. Tew, W. Klopper and J. Gauss, *J. Chem. Phys.*, 2006, **125**, 044108–044108.
- 47 C. Puzzarini, M. Heckert and J. Gauss, *J. Chem. Phys.*, 2008, **128**, 194108–194108.
- 48 CFOUR, a quantum-chemical program package by J.F. Stanton, J. Gauß, M.E. Harding, M.E.P.G. Szalay with contributions from A.A. Auer, R.J. Bartlett, U. Benedikt, C. Berger, D.E. Bernholdt, Y.J. Bomble, L. Cheng, O. Christiansen, M. Heckert, O. Heun, C. Huber, T.-C. Jagau, D. Jonsson, J. Jusélius, K. Klein, W.J. Lauderdale, D.A. Matthews, T. Metzroth, L.A. Mück, D.P. O'Neill, D.R. Price, E. Prochnow, C. Puzzarini, K. Ruud, F. Schiffmann, W. Schwalbach, S. Stopkowicz, A. Tajti, J. Vázquez, F. Wang, J.D. Watts and the integral packages MOLECULE (J. Almlöf and P.R. Taylor), PROPS (P.R. Taylor), ABACUS (T. Helgaker, H.J. Aa. Jensen, P. Jørgensen, and J. Olsen), and ECP routines by A. V. Mitin and C. van Wüllen. For the current version, see <http://www.cfour.de>.
- 49 L. Bizzocchi, C. D. Esposti, L. Dore, J. Gauss and C. Puzzarini, *Mol. Phys.*, 2015, **113**, 801–807.
- 50 E. A. Scarl and F. W. Dalby, *Can. J. Phys.*, 1974, **52**, 1429.
- 51 A. Robinson, J. Brown, J. Flores-Mijangos, L. Zink and M. Jackson, *Mol. Phys.*, 2007, **105**, 639–662.
- 52 J. Gauss and C. Puzzarini, *Mol. Phys.*, 2010, **108**, 269–277.
- 53 K. K. Irikura, *J. Phys. Chem. Ref. Data*, 2007, **36**, 389–397.
- 54 E. Roueff, J. Loison and K. Hickson, *Astron. Astrophys.*, 2015, **576**, A99.

Table 2 Observed frequencies and residuals (in MHz) from the single-isotopologue fit of ^{15}ND in the ground and first vibrational excited states.

State	N'	J'	F_1'	F'	N''	J''	F_1''	F''	Obs. Freq.	Obs.- Calc.	Rel. weight
$v=0$	1	0	0.5	1.5	0	1	0.5	0.5	487528.290(80)	0.119	0.95
	1	0	0.5	0.5	0	1	0.5	0.5	487528.290(80)	0.119	0.05
	1	0	0.5	1.5	0	1	0.5	1.5	487547.166(80)	0.012	0.79
	1	0	0.5	0.5	0	1	0.5	1.5	487547.166(80)	0.012	0.21
	1	0	0.5	1.5	0	1	1.5	1.5	487578.185(500)	-0.229	0.21
	1	0	0.5	0.5	0	1	1.5	1.5	487578.185(500)	-0.229	0.79
	1	0	0.5	1.5	0	1	1.5	2.5	487593.045(500)	-0.332	
	1	2	2.5	3.5	0	1	1.5	2.5	517707.856(50)	0.002	
	1	2	2.5	2.5	0	1	1.5	1.5	517709.082(50)	-0.060	
	1	2	2.5	1.5	0	1	1.5	0.5	517709.837(50)	0.024	
	1	2	1.5	2.5	0	1	0.5	1.5	517712.966(50)	-0.008	
	1	2	2.5	1.5	0	1	1.5	1.5	517721.385(50)	0.046	
	1	2	2.5	2.5	0	1	1.5	2.5	517724.182(50)	0.052	
	1	2	1.5	1.5	0	1	0.5	1.5	517730.725(50)	-0.032	
	1	2	1.5	2.5	0	1	1.5	2.5	517759.241(50)	0.038	
	1	1	0.5	1.5	0	1	0.5	0.5	541723.559(80)	-0.009	0.85
	1	1	0.5	0.5	0	1	0.5	0.5	541723.559(80)	-0.009	0.15
	1	1	0.5	1.5	0	1	0.5	1.5	541742.758(80)	-0.015	0.43
	1	1	0.5	0.5	0	1	0.5	1.5	541742.758(80)	-0.015	0.57
	1	1	1.5	1.5	0	1	0.5	0.5	541751.550(80)	0.064	0.74
	1	1	1.5	0.5	0	1	0.5	0.5	541751.550(80)	0.064	0.26
	1	1	0.5	1.5	0	1	1.5	0.5	541762.512(80)	-0.042	0.31
	1	1	0.5	0.5	0	1	1.5	0.5	541762.512(80)	-0.042	0.69
	1	1	1.5	2.5	0	1	0.5	1.5	541769.817(80)	-0.122	0.98
	1	1	1.5	1.5	0	1	0.5	1.5	541769.817(80)	-0.122	0.02
	1	1	0.5	1.5	0	1	1.5	1.5	541773.823(80)	0.053	0.88
	1	1	0.5	0.5	0	1	1.5	1.5	541773.823(80)	0.053	0.12
	1	1	0.5	1.5	0	1	1.5	2.5	541788.538(80)	-0.154	
	1	1	1.5	1.5	0	1	1.5	0.5	541790.239(80)	-0.069	0.37
	1	1	1.5	0.5	0	1	1.5	0.5	541790.239(80)	-0.069	0.63
	1	1	1.5	2.5	0	1	1.5	1.5	541801.642(80)	-0.006	0.12
	1	1	1.5	1.5	0	1	1.5	1.5	541801.642(80)	-0.006	0.64
	1	1	1.5	0.5	0	1	1.5	1.5	541801.642(80)	-0.006	0.24
	1	1	1.5	2.5	0	1	1.5	2.5	541816.257(80)	0.027	0.84
	1	1	1.5	1.5	0	1	1.5	2.5	541816.257(80)	0.027	0.16
	2	1	1.5	0.5	1	1	0.5	0.5	1009356.833(40)	-0.043	0.78
	2	1	1.5	0.5	1	1	0.5	1.5	1009356.833(40)	-0.043	0.22
	2	3	3.5	3.5	1	2	2.5	2.5	1041497.348(40)	0.028	0.33
	2	3	3.5	4.5	1	2	2.5	3.5	1041497.348(40)	0.028	0.44
	2	3	3.5	2.5	1	2	2.5	1.5	1041497.348(40)	0.028	0.24
	2	3	2.5	2.5	1	2	1.5	1.5	1041499.205(40)	-0.006	0.31
	2	3	2.5	3.5	1	2	1.5	2.5	1041499.205(40)	-0.006	0.50
	2	3	2.5	1.5	1	2	1.5	0.5	1041499.205(40)	-0.006	0.19
	2	3	3.5	2.5	1	2	2.5	2.5	1041510.251(40)	-0.026	0.38
	2	3	2.5	1.5	1	2	1.5	1.5	1041510.251(40)	-0.026	0.62
	2	3	2.5	2.5	1	2	1.5	2.5	1041516.279(40)	-0.058	
	2	3	2.5	3.5	1	2	2.5	3.5	1041550.924(40)	0.018	0.60
	2	3	2.5	1.5	1	2	2.5	1.5	1041550.924(40)	0.018	0.15
	2	3	2.5	2.5	1	2	2.5	2.5	1041550.924(40)	0.018	0.24
	2	2	1.5	1.5	1	1	1.5	0.5	1043854.642(40)	-0.025	0.07
	2	2	1.5	2.5	1	1	1.5	1.5	1043854.642(40)	-0.025	0.08
	2	2	1.5	0.5	1	1	1.5	0.5	1043854.642(40)	-0.025	0.10
	2	2	1.5	1.5	1	1	1.5	1.5	1043854.642(40)	-0.025	0.18
	2	2	1.5	0.5	1	1	1.5	1.5	1043854.642(40)	-0.025	0.08
	2	2	1.5	2.5	1	1	1.5	2.5	1043854.642(40)	-0.025	0.41
	2	2	1.5	1.5	1	1	1.5	2.5	1043854.642(40)	-0.025	0.08
	2	2	2.5	1.5	1	1	1.5	0.5	1043869.811(40)	0.031	0.17
	2	2	2.5	2.5	1	1	1.5	1.5	1043869.811(40)	0.031	0.28
	2	2	2.5	1.5	1	1	1.5	1.5	1043869.811(40)	0.031	0.05
	2	2	2.5	3.5	1	1	1.5	2.5	1043869.811(40)	0.031	0.44
	2	2	2.5	2.5	1	1	1.5	2.5	1043869.811(40)	0.031	0.05
	2	2	2.5	1.5	1	1	1.5	2.5	1043869.811(40)	0.031	0.00
	2	2	1.5	1.5	1	1	0.5	0.5	1043882.279(40)	0.047	0.19
	2	2	1.5	0.5	1	1	0.5	0.5	1043882.279(40)	0.047	0.15
	2	2	1.5	2.5	1	1	0.5	1.5	1043882.279(40)	0.047	0.50
	2	2	1.5	1.5	1	1	0.5	1.5	1043882.279(40)	0.047	0.15
	2	2	1.5	0.5	1	1	0.5	1.5	1043882.279(40)	0.047	0.02
	2	1	0.5	1.5	1	0	0.5	0.5	1063506.127(40)	0.013	0.32
	2	1	0.5	1.5	1	0	0.5	1.5	1063506.127(40)	0.013	0.68
	2	1	1.5	2.5	1	0	0.5	1.5	1063578.610(40)	-0.036	
	2	2	2.5	3.5	1	2	2.5	3.5	1067978.220(40)	0.058	
$v=1$	1	2	2.5	3.5	0	1	1.5	2.5	502775.779(60)	-0.063	
	1	2	2.5	2.5	0	1	1.5	1.5	502777.216(60)	0.054	0.63
	1	2	2.5	1.5	0	1	1.5	0.5	502777.216(60)	0.054	0.37
	1	2	1.5	2.5	0	1	0.5	1.5	502780.683(60)	0.052	
	1	2	2.5	1.5	0	1	1.5	1.5	502789.681(60)	-0.062	0.35
	1	2	1.5	0.5	0	1	0.5	0.5	502789.681(60)	-0.062	0.65
	1	2	2.5	2.5	0	1	1.5	2.5	502792.545(60)	0.031	
	1	2	1.5	1.5	0	1	0.5	1.5	502798.877(60)	0.009	
	1	2	1.5	2.5	0	1	1.5	2.5	502826.422(60)	-0.021	
	1	1	1.5	2.5	0	1	0.5	1.5	526777.091(60)	-0.019	
	1	1	1.5	2.5	0	1	1.5	2.5	526822.941(60)	0.019	

Notes.

Number in parentheses are the experimental uncertainties in units of the last quoted digit. The relative weight is given only for blended transitions.

Table 3 Summary of the data used for the multi-isotopologue fit of imidogen

	Pure rotational			Ro-vibrational		
	no. of lines	no of. vib states	Refs.	no. of lines	no of. bands	Refs.
NH	96	2	Flores-Mijangos <i>et al.</i> ²⁸ , Lewen <i>et al.</i> ²⁹ , TW	451	6	Bernath ³⁰ , Geller <i>et al.</i> ⁸ , Ram and Bernath ²²
ND	144	5	Saito and Goto ³¹ , Takano <i>et al.</i> ³² , Dore <i>et al.</i> ²⁴ , TW	406	6	Ram ³³
¹⁵ NH	61	2	Bailleux <i>et al.</i> ³⁴ , Bizocchi <i>et al.</i> ²³	–	–	
¹⁵ ND	43	2	This work (TW)	–	–	

Table 4 Ro-vibrational Dunham Y_{lm} constants and isotopically invariant U_{lm} parameters determined in the multi-isotopologue fit for imidogen radical

l	m	Y_{lm}		U_{lm}	
		units	value	units	value
1	0	/ cm^{-1}	3282.3629(39)	$\text{cm}^{-1} \text{u}^{1/2}$	3184.2027(35)
2	0	/ cm^{-1}	-78.6810(46)	$\text{cm}^{-1} \text{u}$	-73.9831(43)
3	0	/ cm^{-1}	0.2223(25)	$\text{cm}^{-1} \text{u}^{3/2}$	0.2027(23)
4	0	/ cm^{-1}	-0.02953(68)	$\text{cm}^{-1} \text{u}^2$	-0.02610(60)
5	0	/ cm^{-1}	-0.000263(88)	$\text{cm}^{-1} \text{u}^{5/2}$	-0.000225(75)
6	0	/ cm^{-1}	-0.0001393(45)	$\text{cm}^{-1} \text{u}^{5/2}$	-0.0001158(37)
0	1	/ MHz	499690.529(84)	$\text{cm}^{-1} \text{u}$	15.7043731(39)
1	1	/ MHz	-19494.41(34)	$\text{cm}^{-1} \text{u}^{3/2}$	-0.593919(10)
2	1	/ MHz	67.19(48)	$\text{cm}^{-1} \text{u}^2$	0.001981(14)
3	1	/ MHz	-7.69(31)	$\text{cm}^{-1} \text{u}^{5/2}$	$-2.201(87) \times 10^{-4}$
4	1	/ MHz	-1.579(94)	$\text{cm}^{-1} \text{u}^3$	$-4.37(26) \times 10^{-5}$
5	1	/ MHz	0.130(14)	$\text{cm}^{-1} \text{u}^{7/2}$	$3.48(37) \times 10^{-6}$
6	1	/ MHz	-0.01456(76)	$\text{cm}^{-1} \text{u}^{7/2}$	$-3.79(20) \times 10^{-7}$
0	2	/ MHz	-51.44722(91)	$\text{cm}^{-1} \text{u}^2$	-0.00152786(15)
1	2	/ MHz	0.8253(24)	$\text{cm}^{-1} \text{u}^{5/2}$	$2.3594(68) \times 10^{-5}$
2	2	/ MHz	-0.0642(15)	$\text{cm}^{-1} \text{u}^3$	$-1.779(42) \times 10^{-6}$
3	2	/ MHz	0.00269(37)	$\text{cm}^{-1} \text{u}^{7/2}$	$7.24(99) \times 10^{-8}$
4	2	/ MHz	-0.001460(28)	$\text{cm}^{-1} \text{u}^4$	$-3.806(72) \times 10^{-8}$
0	3	/ MHz	0.0037950(79)	$\text{cm}^{-1} \text{u}^3$	$1.0931(36) \times 10^{-7}$
1	3	/ MHz	$-1.339(45) \times 10^{-4}$	$\text{cm}^{-1} \text{u}^{7/2}$	$-3.60(12) \times 10^{-9}$
2	3	/ MHz	$-1.25(18) \times 10^{-5}$	$\text{cm}^{-1} \text{u}^4$	$-3.26(47) \times 10^{-10}$
3	3	/ MHz	$-4.26(31) \times 10^{-6}$	$\text{cm}^{-1} \text{u}^{9/2}$	$-1.075(79) \times 10^{-10}$
0	4	/ MHz	$-4.47(16) \times 10^{-7}$	$\text{cm}^{-1} \text{u}^4$	$-1.166(42) \times 10^{-11}$
1	4	/ MHz	$-3.49(29) \times 10^{-8}$	$\text{cm}^{-1} \text{u}^{9/2}$	$-8.80(74) \times 10^{-13}$
0	5	/ MHz	$3.72(88) \times 10^{-11}$	$\text{cm}^{-1} \text{u}^{9/2}$	$9.1(22) \times 10^{-16}$
X	l	m	δ_{lm}^X	Δ_{lm}^X	
N	0	1	/ MHz	75.71(11)	-3.8592(58)
N	1	1	/ MHz	-3.45(13)	-4.50(17)
H	1	0	/ cm^{-1}	1.6117(14)	-0.90162(78)
H	2	0	/ cm^{-1}	-0.01098(24)	-0.2565(55)
H	0	1	/ MHz	1005.124(35)	-3.68744(13)
H	1	1	/ MHz	-0.3733(47)	-3.2030(29)
H	0	2	/ MHz	-34.054(31)	-13.23(17)
H	0	3	/ MHz	$1.48(11) \times 10^{-4}$	-69.1(51)

Notes.

The Dunham constants Y_{lm} are referred to the most abundant NH isotopologue. The BOB coefficients Δ_{lm}^X are adimensional. Number in parentheses are the 1σ statistical errors in units of the last quoted digit.

Table 5 Fine and hyperfine Dunham \mathcal{Y}_{im} constants and isotopically invariant $U_{im}^{\mathcal{Y}}$ parameters determined in the multi-isotopologue fit for NH

Dunham type			Isotopically invariant		
Fine structure parameters					
λ_{00}	/ MHz	27573.424(23)	U_{00}^{λ}	/ MHz u	0.9174536(52)
λ_{10}	/ MHz	16.200(46)	U_{10}^{λ}	/ MHz $u^{1/2}$	$5.864(20) \times 10^{-4}$
λ_{20}	/ MHz	-14.645(22)	U_{20}^{λ}	/ MHz u	$-4.5922(68) \times 10^{-4}$
λ_{01}	/ MHz	0.0109(38)	U_{01}^{λ}	/ MHz $u^{3/2}$	$3.4(12) \times 10^{-7}$
γ_{00}	/ MHz	-1688.280(31)	U_{00}^{γ}	/ MHz u	-0.0528438(13)
γ_{10}	/ MHz	88.172(93)	U_{10}^{γ}	/ MHz $u^{3/2}$	0.0026750(27)
γ_{20}	/ MHz	-1.387(79)	U_{20}^{γ}	/ MHz $u^{3/2}$	$-4.06(23) \times 10^{-5}$
γ_{30}	/ MHz	0.370(21)	U_{30}^{γ}	/ MHz $u^{3/2}$	$1.054(61) \times 10^{-5}$
γ_{01}	/ MHz	0.4631(31)	U_{01}^{γ}	/ MHz u^2	$1.3656(91) \times 10^{-5}$
γ_{11}	/ MHz	-0.0291(81)	U_{11}^{γ}	/ MHz $u^{3/2}$	$-8.4(23) \times 10^{-7}$
γ_{21}	/ MHz	0.0152(45)	U_{21}^{γ}	/ MHz u^2	$4.2(13) \times 10^{-7}$
γ_{31}	/ MHz	-0.00333(72)	U_{31}^{γ}	/ MHz u^2	$-9.0(19) \times 10^{-8}$
$\delta_{00}^{\lambda,N}$	/ MHz	-3.59(16)	$\Delta_{00}^{\lambda,N}$		0.837(37)
$\delta_{00}^{\lambda,H}$	/ MHz	-65.250(40)	$\Delta_{00}^{\lambda,H}$		1.08957(67)
$\delta_{10}^{\lambda,H}$	/ MHz	1.934(40)	$\Delta_{10}^{\lambda,H}$		-49.0(10)
$\delta_{00}^{\gamma,H}$	/ MHz	1.712(18)	$\Delta_{00}^{\gamma,H}$		3.515(38)
$\delta_{10}^{\gamma,H}$	/ MHz	-0.091(17)	$\Delta_{10}^{\gamma,H}$		3.83(66)
Hyperfine structure parameters					
$b_{F,00}(H)$	MHz	-64.194(13)	$U_{00}^{bF}(H)$	cm^{-1}	-0.00214129(45)
$b_{F,10}(H)$	MHz	-3.785(15)	$U_{10}^{bF}(H)$	cm^{-1}	$-1.2243(48) \times 10^{-4}$
$c_{00}(H)$	MHz	92.216(61)	$U_{00}^c(H)$	cm^{-1}	0.0030760(20)
$c_{10}(H)$	MHz	-3.391(58)	$U_{10}^c(H)$	cm^{-1}	$-1.097(19) \times 10^{-4}$
$C_{00}(H)$	MHz	-0.068(11)	$U_{00}^C(H)$	cm^{-1}	$-2.14(33) \times 10^{-6}$
$b_{F,00}(D)$	MHz	-9.836(12)	$U_{00}^{bF}(D)$	cm^{-1}	$-3.2810(41) \times 10^{-4}$
$b_{F,10}(D)$	MHz	-0.632(10)	$U_{10}^{bF}(D)$	$\text{cm}^{-1} u^{1/2}$	$-2.044(34) \times 10^{-5}$
$c_{00}(D)$	MHz	14.233(74)	$U_{00}^c(D)$	cm^{-1}	$4.746(25) \times 10^{-4}$
$c_{10}(D)$	MHz	-0.372(99)	$U_{10}^c(D)$	$\text{cm}^{-1} u^{1/2}$	$-1.19(32) \times 10^{-5}$
$c_{20}(D)$	MHz	-0.117(32)	$U_{20}^c(D)$	$\text{cm}^{-1} u^{1/2}$	$-3.66(100) \times 10^{-6}$
$eQe_{00}(D)$	MHz	0.080(32)	$U_{00}^{eQe}(D)$	cm^{-1}	$2.7(11) \times 10^{-6}$
$b_{F,00}(^{14}\text{N})$	MHz	19.084(18)	$U_{00}^{bF}(^{14}\text{N})$	cm^{-1}	$6.3660(59) \times 10^{-4}$
$b_{F,10}(^{14}\text{N})$	MHz	-0.421(31)	$U_{10}^{bF}(^{14}\text{N})$	$\text{cm}^{-1} u^{1/2}$	$-1.365(99) \times 10^{-5}$
$b_{F,20}(^{14}\text{N})$	MHz	-0.088(13)	$U_{20}^{bF}(^{14}\text{N})$	$\text{cm}^{-1} u^{1/2}$	$-2.76(41) \times 10^{-6}$
$c_{00}(^{14}\text{N})$	MHz	-68.135(31)	$U_{00}^c(^{14}\text{N})$	$\text{cm}^{-1} u^{1/2}$	-0.0022727(10)
$c_{10}(^{14}\text{N})$	MHz	0.467(26)	$U_{10}^c(^{14}\text{N})$	$\text{cm}^{-1} u^{3/2}$	$1.509(83) \times 10^{-5}$
$eQq_{00}(^{14}\text{N})$	MHz	-3.367(54)	$U_{00}^{eQq}(^{14}\text{N})$	cm^{-1}	$-1.123(18) \times 10^{-4}$
$eQq_{10}(^{14}\text{N})$	MHz	0.395(38)	$U_{10}^{eQq}(^{14}\text{N})$	$\text{cm}^{-1} u^{1/2}$	$1.28(12) \times 10^{-5}$
$C_{00}(^{14}\text{N})$	MHz	0.172(11)	$U_{00}^C(^{14}\text{N})$	$\text{cm}^{-1} u^{1/2}$	$5.42(36) \times 10^{-6}$
$C_{10}(^{14}\text{N})$	kHz	-0.0293(85)	$U_{10}^C(^{14}\text{N})$	$\text{cm}^{-1} u^{3/2}$	$-9.0(26) \times 10^{-7}$
$b_{F,00}(^{15}\text{N})$	MHz	-26.848(16)	$U_{00}^{bF}(^{15}\text{N})$	cm^{-1}	$-8.9556(52) \times 10^{-4}$
$b_{F,10}(^{15}\text{N})$	MHz	0.860(18)	$U_{10}^{bF}(^{15}\text{N})$	$\text{cm}^{-1} u^{1/2}$	$2.789(58) \times 10^{-5}$
$c_{00}(^{15}\text{N})$	MHz	95.428(49)	$U_{00}^c(^{15}\text{N})$	cm^{-1}	0.0031831(16)
$c_{10}(^{15}\text{N})$	MHz	-0.556(54)	$U_{10}^c(^{15}\text{N})$	cm^{-1}	$-1.80(17) \times 10^{-5}$
$C_{00}(^{15}\text{N})$	MHz	-0.259(22)	$U_{00}^C(^{15}\text{N})$	$\text{cm}^{-1} u^{1/2}$	$-8.18(71) \times 10^{-6}$
$C_{10}(^{15}\text{N})$	MHz	0.099(24)	$U_{10}^C(^{15}\text{N})$	$\text{cm}^{-1} u^{1/2}$	$3.06(74) \times 10^{-6}$

Notes.

The Dunham constants \mathcal{Y}_{im} are referred to the most abundant NH isotopologue. The BOB coefficients Δ_{im}^X are adimensional. Number in parentheses are the 1σ statistical errors in units of the last quoted digit.

Table 6 Born–Oppenheimer and equilibrium bond distances (in pm) from the individual isotopologues (see text).

Species	r_e	$r_e - r_e^{\text{BO}}$
NH	103.716377(16)	0.109656
¹⁵ NH	103.715864(16)	0.109143
ND	103.665420(10)	0.058699
¹⁵ ND	103.664908(10)	0.058187
$r_e^{\text{BO}} = 103.606721(13)$		
$r_e^{\text{theor}} = 103.5915$		

Table 7 Contributions of the Born–Oppenheimer Breakdown coefficients to the U_{01} constant

Atom	$\Delta_{01}(\text{exp})$	adiabatic	non-adiabatic	Dunham
N	-3.8592	-0.6515	-3.1326	-0.0751
H	-3.6874	-1.0379	-2.5744	-0.0751

Table 8 Zero Point Energies (in cm^{-1}) of imidogen isotopologues.

Species	This work	Ref. 53	Ref. 54
NH	1623.5359(17)	1623.6(6)	1621.5 ^a
¹⁵ NH	1619.9485(17)		1617.9 ^b
ND	1190.0859(11)	1190.13(5)	1189.5 ^c
¹⁵ ND	1185.1413(11)		1183.6 ^b

Notes.

Number in parentheses are the 1σ statistical errors in unit of the last quoted digit. ^(a) From Ref. 22. ^(b) Computed. ^(c) From Ref. 24.